NRL Report 6913

Coupling of Fracture Mechanics and Transition Temperature Approaches to Fracture-Safe Design

F. J. Loss and W. S. Pellini

Reactor Materials Branch
Metallurgy Division

April 14, 1969

NAVAL RESEARCH LABORATORY
Washington, D.C.

This document has been approved for public release and sale; its distribution is unlimited.

CONTENTS

Abstract	ii
Problem Status	ii
Authorization	ii
NOMENCLATURE	1
INTRODUCTION	2
CONCEPT OF THE LIMITING TRANSITION FOR DYNAMIC FRACTURE PROPAGATION	4
DT TEST DEFINITION OF LTTR	6
THICK SECTION DT TESTS FOR SIZE-EFFECT STUDIES	8
COMPARISON OF FRACTURE MECHANICS AND DT TESTS	17
FRACTURE MECHANICS INTERPRETATIONS OF NDT	19
THICKNESS EFFECTS INTERPRETATIONS OF THE FAD	21
FAD APPLICATION TO PRESSURE VESSELS INVOLVING GEOMETRIC INSTABILITY	24
SUMMARY	26
REFERENCES	27

ABSTRACT

The effect of mechanical constraint on the transition temperature features for steels of thick section is examined in the framework of linear elastic fracture mechanics K_{Ic} and K_{Id} tests and the Dynamic Tear (DT) test. It is demonstrated that steels of fracture toughness and yield strength levels representative of the A533-B type continue to exhibit a transition to high fracture toughness in thick sections. The distinguishing feature of thick sections is a size effect involving a shift of the transition temperature midpoint on the order of 60°F. The DT test defines a limiting transition temperature region, which can be divided into three parts: a low temperature regime in which plane strain fracture mechanics is applicable, a higher temperature regime which is beyond the limits of fracture mechanics definition and is relatable to crack arrest conditions of the FTE type, and a final regime involving large plastic deformation in association with the fracture. The relatively narrow temperature span of the plane strain regime above the NDT temperature indicates practical difficulties in the direct application of fracture mechanics tests due to requirements for K_{Ic} and K_{Id} test specimens of large dimensions. A practical solution to the use of fracture mechanics principles may be obtained by considering the temperature-dependence aspects of the K_{Ic} and K_{Id} parameters. In general, the applicability of this approach is limited to temperatures below the FTE. If structural operation cannot be confined to temperatures above FTE, the Fracture Analysis Diagram (FAD) procedure, which is now extended to thick sections, is recommended as the best available engineering approach. The Drop Weight-NDT and FAD procedures are analyzed in terms of fracture mechanics aspects.

PROBLEM STATUS

This is a special interpretative report aimed at the general problem of fracture-safe design. The major portion of the studies is continuing under the established problem.

AUTHORIZATION

NRL Problem M01-14
RR 007-01-46-5409
AEC-83Y-80507V
and
NRL Problem M01-25
RR 007-01-46-5432

Manuscript submitted March 18, 1969.

COUPLING OF FRACTURE MECHANICS AND TRANSITION TEMPERATURE APPROACHES TO FRACTURE-SAFE DESIGN

NOMENCLATURE

B	thickness of specimen or structural section (in.)
σ_{ys}	yield stress for static (slow) loading (ksi)
σ_{yd}	yield stress for dynamic loading (ksi)
K_{Ic}	static (slow load) plane strain fracture toughness (ksi$\sqrt{\text{in.}}$)
K_{Id}	dynamic plane strain fracture toughness (ksi $\sqrt{\text{in.}}$)
CAT	Crack Arrest Temperature determined with the Robertson test; also indexed by regime 1 of the DT test
CTS	compact K_{Ic} specimen
DT	Dynamic Tear
E/A	energy per unit fracture area of DT specimen (ft-lb/in.^{2})
FAD	Fracture Analysis Diagram
FTE	Fracture Transition Elastic
FTP	Fracture Transition Plastic
GI	geometric instability relating to the bulging of pressure vessels
LEFM	linear elastic fracture mechanics
LTTR	Limiting Transition Temperature Range as defined by dynamic fracture propagation tests
NDT	Nil Ductility Transition temperature obtained by the Drop Weight Test (DWT)
Regime 1	transition temperature range of initial gradual increase of microfracture and macrofracture ductility
Regime 2	transition temperature range of rapid increase of microfracture and macrofracture ductility
Regime 3	transition temperature range of completion of microfracture and macrofracture ductility transition
RW	longitudinal specimen (i.e., strong fracture orientation)
WR	transverse specimen (i.e., weak fracture orientation)

INTRODUCTION

For several decades transition temperature methods have been the primary approach to fracture-safe design for engineering structures. This approach has manifested itself in various transition temperature tests, such as the Robertson, Drop Weight, Charpy-V, Drop Weight Tear, and Double Tension. These methods have been applied to steels of low strength and high shelf level toughness, which exhibit a change in the nature of the fracture propagation from unstable (brittle) to stable (ductile) modes in a relatively narrow temperature increment.

With the introduction of ultra high strength steels, which generally do not exhibit a transition temperature behavior, new approaches had to be developed to cope with structural failures. Fracture mechanics represents a new discipline to deal with such materials. The analytical aspects of this approach provide a highly desirable ability to predict the critical crack size-stress level relation for any material condition, for which the plane strain fracture toughness K_{Ic} and K_{Id} can be measured. However, the primary application of fracture mechanics is to materials of relatively brittle characteristics.

Within the last 10 years NRL developed new interpretative approaches, using the Dynamic Tear (DT) test, to investigate the fracture characteristics of nontransition temperature materials, such as ultra high strength steel and nonferrous alloys (1,2). This method is also applicable to transition temperature steels and may be scaled to investigate the effects of section size on fracture toughness, for either the nontransition or temperature transition aspects of fracture.

The increasing application of thick sections in large engineering structures has necessitated an evaluation of the fracture safety of steels used for this purpose. The thick-section designs generally use steels which are known to exhibit a transition temperature behavior in thin sections. On the basis of evidence evolved from structural failures it had been proposed that unstable fracture could be prevented by service operation in excess of NDT + 60°F for steels of thin sections. The Fracture Analysis Diagram (FAD) interpretative procedure (3) locates the FTE (equivalent to the CAT for yield point loading) point at this relative temperature. The applicable FTE temperature for the case of very thick sections has remained in question; however, the general premise derived from metallurgical concepts was that the section-size effect should be relatively small.

Fracture mechanics theory presented a challenge to this concept. In attempting to apply fracture mechanics procedures to the low-alloy transition temperature steels, K_{Ic} values were obtained at temperatures up to the NDT with reasonable size specimens (1 to 2 in. thick), as shown in Fig. 1 for A533-B steel. It was postulated that the reason valid data could not be obtained at higher temperatures with these specimens was the loss of mechanical constraint at the crack tip. This resulted in an inability to maintain plane strain conditions. Since the constraint at the crack tip is related to section thickness, it was presumed that thicker sections would provide the required constraint, thereby enabling valid K_{Ic} values to be obtained at much higher temperatures.* This hypothesis projects a gradual rise in toughness with temperature as shown in Fig. 1. The alarming consequence of the projected slow rise in toughness with temperature is that it presents the possibility of brittle fracture resulting from elastic loading for flaws located in thick sections, at temperatures believed to guarantee fracture safety. The projected level of fracture toughness, as deduced from a K_{Ic}/σ_{ys} ratio equal to 2.0 in the 300 to 400°F range, indicates that brittle (plane strain) fractures can be obtained in plates of 10-in. or greater thickness. If this were true, a sharp temperature transition in fracture toughness would not be developed for thick sections.

---

*The required thickness B to measure a given fracture toughness expressed as the ratio K_{Ic}/σ_{ys} is computed from the relation recommended by ASTM Committee E-24 as follows: $B \geq 2.5\,(K_{Ic}/\sigma_{ys})^2$.

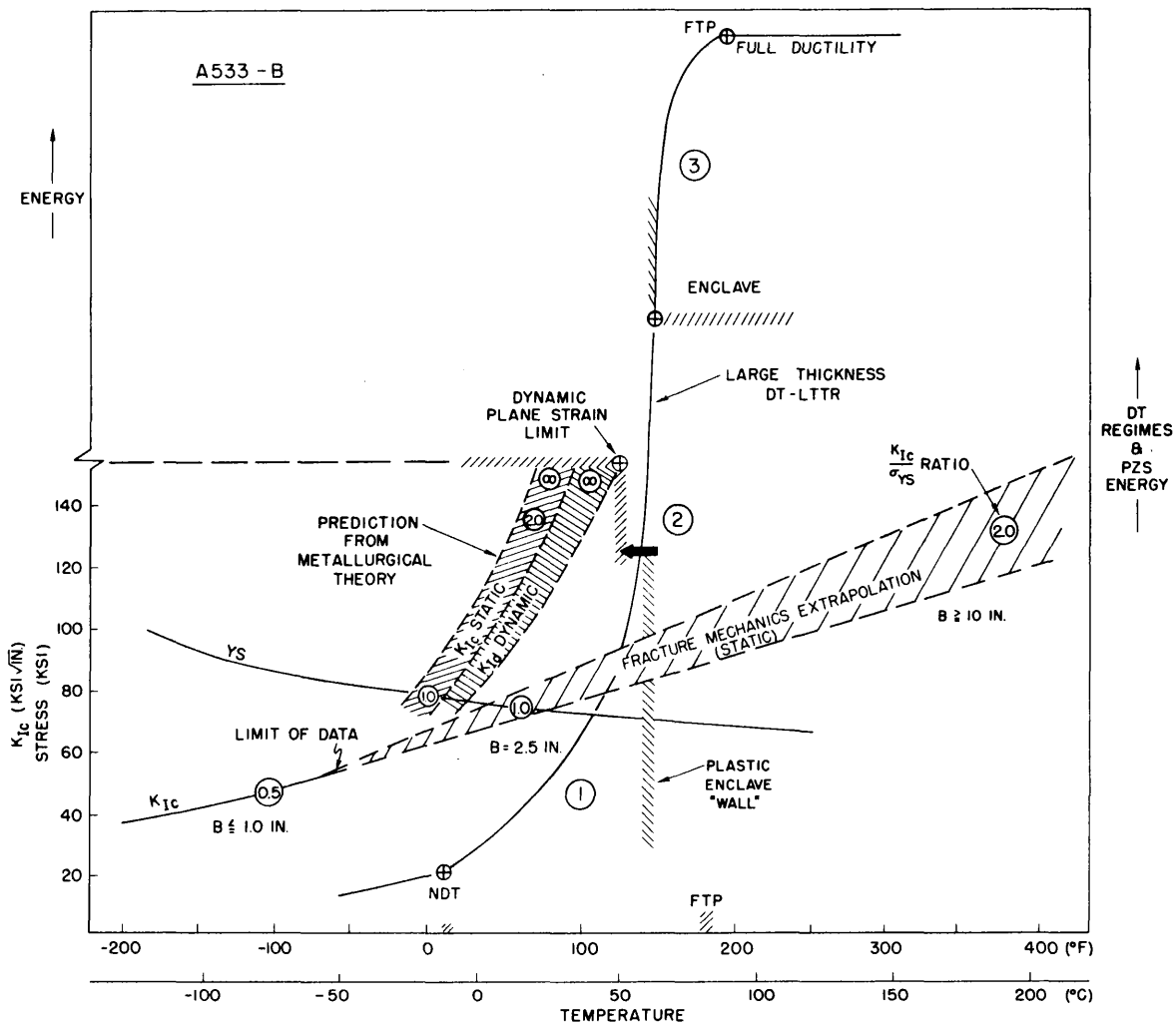

Fig. 1 - Nature of the conflict between predictions based on metallurgical and fracture mechanics concepts as to the effects of large thickness on plane strain fracture toughness. Fracture mechanics extrapolations from low temperatures predicted retention of plane strain (brittle fracture) to high temperatures. Metallurgical considerations predicted a sharp rise of K_{Ic} and K_{Id} values at temperatures above NDT. The bold arrow signifies that the transition to plastic fracture (enclave) serves as a temperature "wall" barrier to the development of plane strain fracture.

On the other hand, metallurgical concepts predict a transition temperature behavior for the thick sections due to the basic effects of temperature on microfracture processes. The predictions of the metallurgical theory include a temperature increase of the transition range for heavy sections but only by a nominal amount. This prediction is indicated in Fig. 1 by the temperature scale location of the sharp increase in fracture toughness for A533-B steel as measured by thick-section DT tests. The temperature effect should result in a correspondingly sharp upsweep in the static K_{Ic}/σ_{ys} and dynamic K_{Id}/σ_{yd} ratios, which are the fracture mechanics index parameters of fracture toughness. These ratios should become unmeasurably high (infinity) at temperatures lower than the transition region defined by the large-size DT test specimens.

If the fracture mechanics prediction is correct, it would result in serious consequences to the operation of thick-walled pressure vessels. It is evident from the fracture mechanics predictions of Fig. 1 that NDT + 60°F would not ensure the considerable increase in toughness and corresponding decrease in the probability of fracture initiation that is normally expected above the NDT temperature.

An experimental program was undertaken to answer these questions. In collaboration with the U.S. Atomic Energy Commission, Heavy Section Steel Technology (HSST) Program, NRL conducted large-scale DT tests (12 in. thick) on A533-B reactor pressure vessel steel supplied by the HSST Program. Other investigations on 6-in.-thick A533-B plate were already underway at NRL. The Westinghouse Research Laboratories conducted 12-in. compact tension (CTS) fracture mechanics tests of this same HSST material. In this way both points of view on the effect of mechanical constraint were investigated.

CONCEPT OF THE LIMITING TRANSITION FOR DYNAMIC FRACTURE PROPAGATION

The transition features of dynamic fracture propagation tests have been considered to represent the highest temperature range for the brittle-to-ductile transition of cleavage fracture. This limiting transition temperature range (LTTR) is defined by the change in the nature of fracture propagation from unstable (brittle) to stable (ductile) modes. At the low-temperature end of the transition the release of elastic strain energy in an increment of crack propagation is sufficient to provide the energy required for the next increment of propagation; accordingly, the fracture is of the unstable, brittle type. In the course of the transition the microductility of the metal becomes too high to permit fracture extension by the release of elastic strain energy alone. At the high end of the transition the fracture must be propagated by ductile tearing processes.

The microscale events for the temperature transition may be explained in terms of the competing processes of cleavage and slip. At temperatures where the cleavage stress of individual grains is lower than the stress for yielding (slip), the resultant cleavage fracture is of the stress-induced (brittle) type. Above a critical temperature, extensive slip (yielding) occurs first, and the crystals develop plastic strain, which elevates the flow stress (by work hardening) to the level of the cleavage stress. The resultant cleavage fracture is then of the strain-induced (ductile) type. The change from stress- to strain-induced cleavage fracture marks the beginning of a transition which is reflected on macroscopic as well as microscopic scales. This initial region of the transition will be referred to as regime 1 for both scale levels. The plastic strain associated with strain-induced cleavage fracture increases sharply with increase in temperature, and the transition then enters a stage defined as regime 2. Following the sharp rise, the ductility increase continues as the number of isolated grain microcleavages falls to very low levels. At this point they can never be joined to form an unstable cleavage crack. Fully fibrous fracture therefore develops at this point, and the transition reaches an upper shelf energy limit. The important point to be noted here is that the appearance of cleavage on fracture surfaces is not necessarily indicative of brittle fracture, because a large plastic strain may be involved prior to metal separation by cleavage.

The transitions in microfracture ductility are reflected on a macroscopic scale by increased fracture toughness of laboratory tests and in the fracture resistance of the metal in structures. Figure 2 illustrates the general course of macroscopic scale events for the case of deep, sharp cracks subjected to slow (static) and dynamic loading. Regime 1 of the transition for static loading denotes an increase in plane strain fracture toughness, which requires increased mechanical constraint (increased B thickness) to suppress the development of a K_{Ic} to K_c (mixed-mode) transition. The fact that

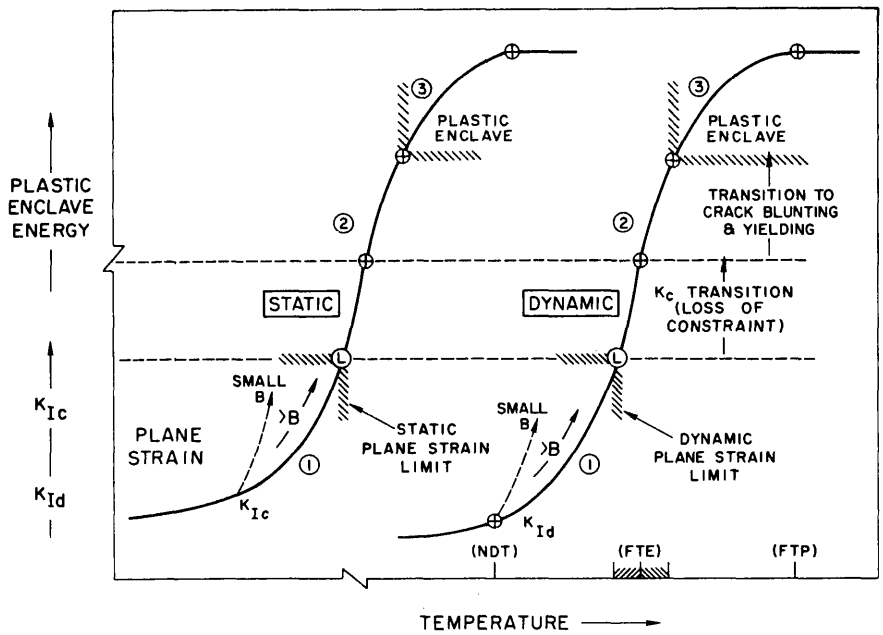

Fig. 2 - Metallurgical concepts illustrating that the transition through the three regimes of microfracture ductility should result in parallel macrofracture transitions. The degree of mechanical constraint and strain rate at the crack tip determines the temperature for starting the regime 1 microfracture transition and therefore the starting of the macroscopic transition. Once started, the respective transitions run their full course and cannot be forced (mechanically) to remain in the regime 1 state.

increased constraint is required to suppress K_c behavior with increasing temperatures is a certain sign that significant increases in microfracture ductility are evolving due to the increase in temperature. The increased thickness provides increased constraint to expand the temperature range of the plane strain condition, but it would seem that there is a limit to which added constraint can suppress the temperature-induced increase in microfracture ductility. The K_{Ic} rise through regime 1 is illustrated in Fig. 2 to reach a limit for which increased thickness is no longer sufficient to ensure plane strain constraint at the crack tip. This limit marks the end of regime 1 and also the end of the plane strain state.

The transition from regime 1 to regime 2 involves a K_{Ic} to K_c transition, due to the loss of constraint enforced by high intrinsic ductility of the metal. As this constraint barrier is breached, the subsequent rapid increase in microfracture ductility with increased temperature has a dramatic effect on macroscopic fracture toughness. The transition through regime 2 also involves the development of extensive yielding of the material surrounding the crack tip, which causes crack tip blunting. This final process rapidly elevates the fracture transition to completion in regime 3, where fully ductile fracture is achieved. The extreme plastic deformation required to propagate the fracture in regime 3 can be compared to the high degree of plastic strain prior to forming a tensile neck and will be referred to as a "plastic enclave."

The static transition can be raised to higher temperatures by the effects of increased rate of loading on the plastic flow stress. When all factors relating to sharpness of cracks, increased thickness, and dynamic loading have been introduced, a final transition

temperature range emerges which cannot be breached, because it is limit controlled by microfracture ductility - this is the LTTR. Any point on the curve defining the LTTR signifies a fracture mode which cannot proceed by a lower energy process. For example, regime 3 of the LTTR which relates to a fully fibrous fracture means that a lower energy process such as cleavage is impossible under any set of crack tip, constraint, and loading conditions. However, regime 1 which relates to brittle fracture can emerge as involving high ductility, for mechanical conditions less severe than those specified for the LTTR.

DT TEST DEFINITION OF LTTR

The transition defined by the DT test is considered to represent the LTTR, since this test features all of the elements required to impose the limiting (maximum severity) mechanical conditions. The DT specimen usually features a brittle electron beam crack starter weld, which provides the equivalent of a deep sharp notch. Small-size DT specimens may be prepared by machining and sharpening of the notch with a knife edge. The DT test is conducted by dynamic loading, never by static loading. The specimen geometries for the 1-in. and 5/8-in. DT specimens are shown in Fig. 3. Descriptions of the test procedures are given in Ref. 4. The general shape of the DT test energy curve for transition metals of high shelf toughness is indicated by the dynamic case curve of Fig. 2. The three regimes shown can be approximated from the DT test energy transition curve by dividing the total curve into three equal sections according to energy. This definition evolves from experimental evidence of the fractured surfaces and suffices for engineering use when the total transition occurs over a narrow temperature interval, as is the case for steels of high shelf energy.

From the fracture appearance and lateral dimpling observed in both thin and thick section DT tests, it can be proven that the limit of fracture propagation under purely elastic loads must lie within regime 2. The energy curve midpoint is selected as a convenient reference. Since the transition through regime 2 is very steep, little difference will result in the index temperature by changing the reference point in this regime. The midpoint reference temperature is considered to correspond to the FTE point of the FAD (3). This means that stresses above yield level would be required to propagate dynamic fractures above the FTE index temperature. It also implies that dynamic K_{Ic} (i.e., K_{Id}) values will not be obtainable beyond this index point, as a conservative upper temperature bound.

The beginning of the energy rise in regime 1 of the DT test is invariantly indexed to the Drop Weight Test-NDT (DWT-NDT) temperature, because the NDT temperature indicates the beginning of a rapid increase in microfracture ductility for the case of dynamic loading. The slope of the DT energy curve in regime 1 may be expected to change as a function of thickness, but the NDT point, which marks the beginning of the rapid energy increase, will remain invariant. The full significance of NDT is further discussed in fracture mechanics terms in a subsequent section.

Regime 1 of the DT test corresponds to the CAT curve as determined by the Robertson test. This feature may not be obvious, since the CAT is normally indexed by stress and the DT curve is indexed by energy; Fig. 4 serves to clarify the comparison. The figure shows the results of 5/8-in. DT tests for two 1-in.-thick pressure vessel steels. The FTE temperatures are indexed by the DT test energy curves at their midpoints. The Robertson toe regions are indexed by the respective NDT temperatures. The upper portion of Fig. 4 shows the two estimated CAT curves as drawn between the index points of NDT and FTE of the two steels. Robertson data from tests conducted by the UK Reactor Materials Laboratory at Culcheth, England, are shown to provide a good verification of the predicted CAT for 0.5 yield stress loading for both steels.

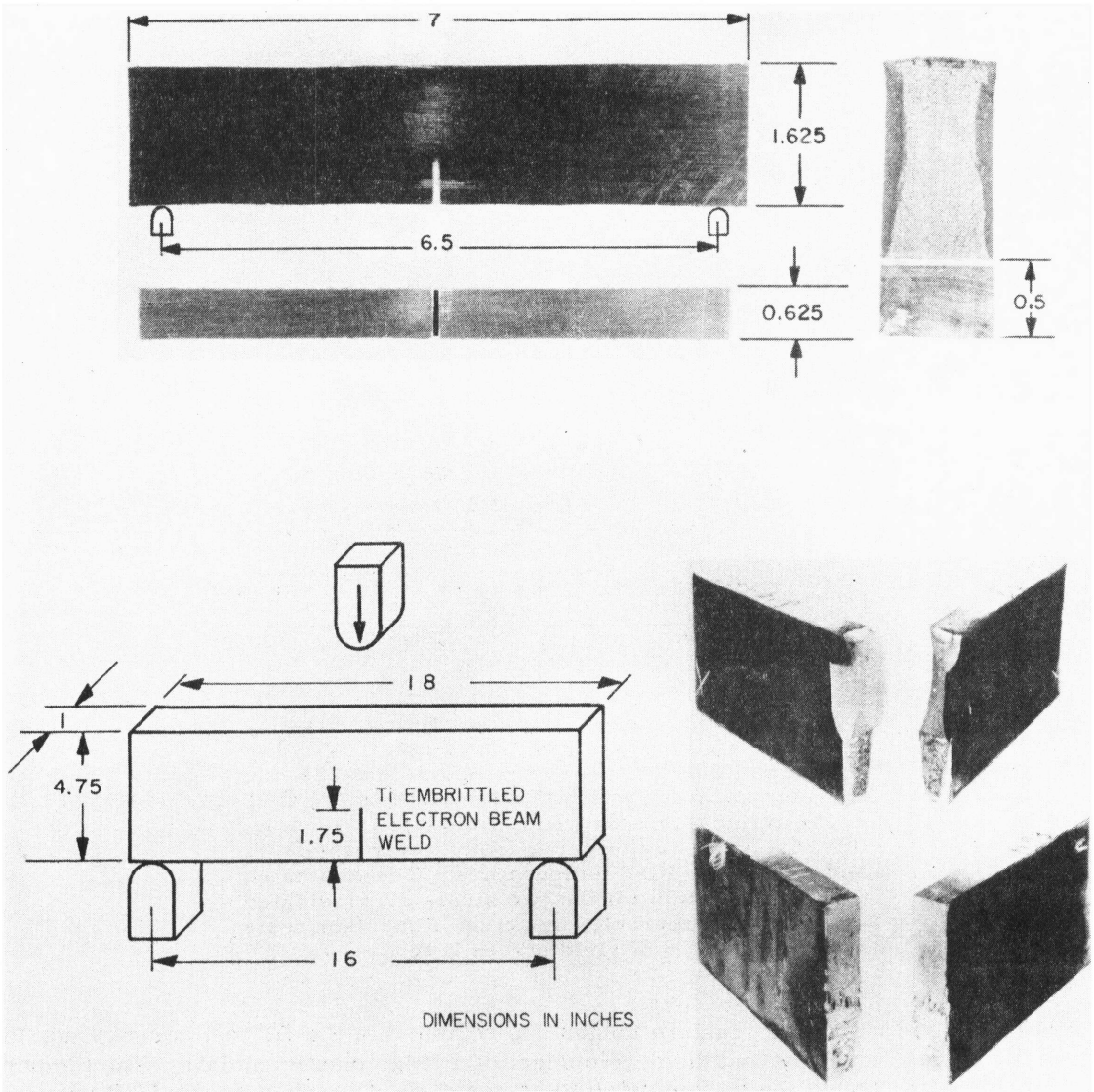

Fig. 3 - Features of 5/8-in. and 1-in. DT specimens. The 5/8-in. DT (top) is shown featuring the machined slot, with a knife-edge sharpened, notch tip. The 1-in. DT (bottom) features the brittle electron beam weld which is also used for the 5/8-in. DT, as desired. The broken halves of the 1-in. DT specimens illustrate brittle- and ductile-type fractures.

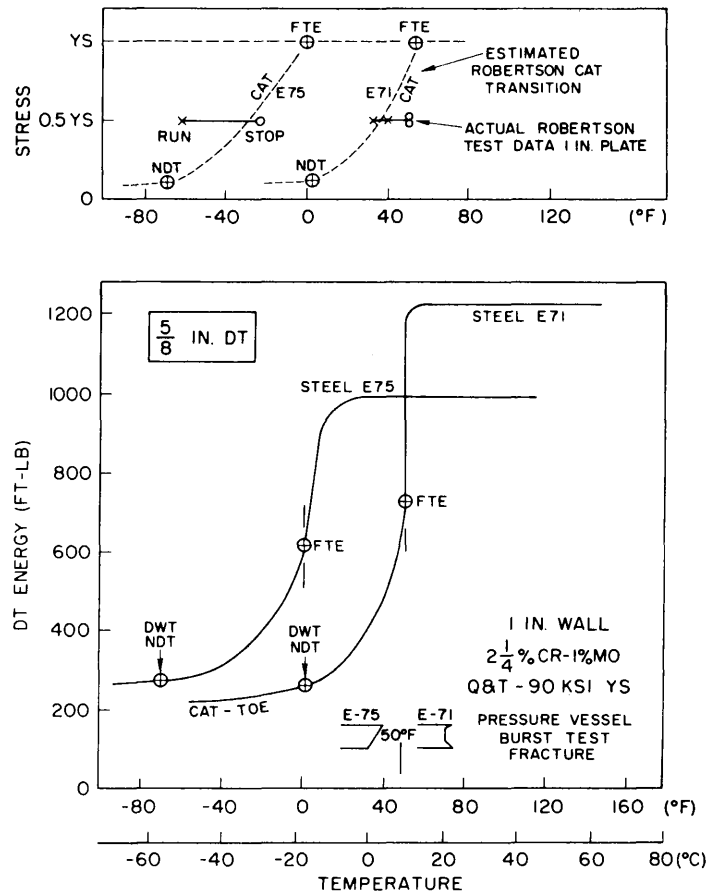

Fig. 4 - DT test indexing procedures for estimating the temperature scale position of the CAT curve (bottom). The DT energy midpoint indexes the FTE temperature which is equivalent to the CAT curve arrest temperature for yield stress loading. The CAT toe region (rise from lower shelf) is indexed to the NDT temperature. The estimated CAT curves (top) for the two steels are indicated to be located correctly by actual Robertson tests conducted at 0.5 of yield stress level.

For steels of high shelf fracture toughness, regime 3 of the DT test corresponds to gross plastic load stresses and the development of a large plastic enclave. The temperature at which the transition is completed to an upper shelf is taken as the FTP reference point, as defined in earlier reports (3,5).

THICK SECTION DT TESTS FOR SIZE-EFFECT STUDIES

Since the DT test can be scaled to any thickness of interest as shown in Fig. 5 and Table 1, it provides a simple and unique method for investigating theoretical predictions as to the effect of mechanical constraint on fracture toughness. If plane strain conditions are retained to high temperatures by large section size, this fact should be demonstrated by the large DT tests. Evidence that the three regimes of the LTTR are not eliminated would indicate control by microfracture ductility.

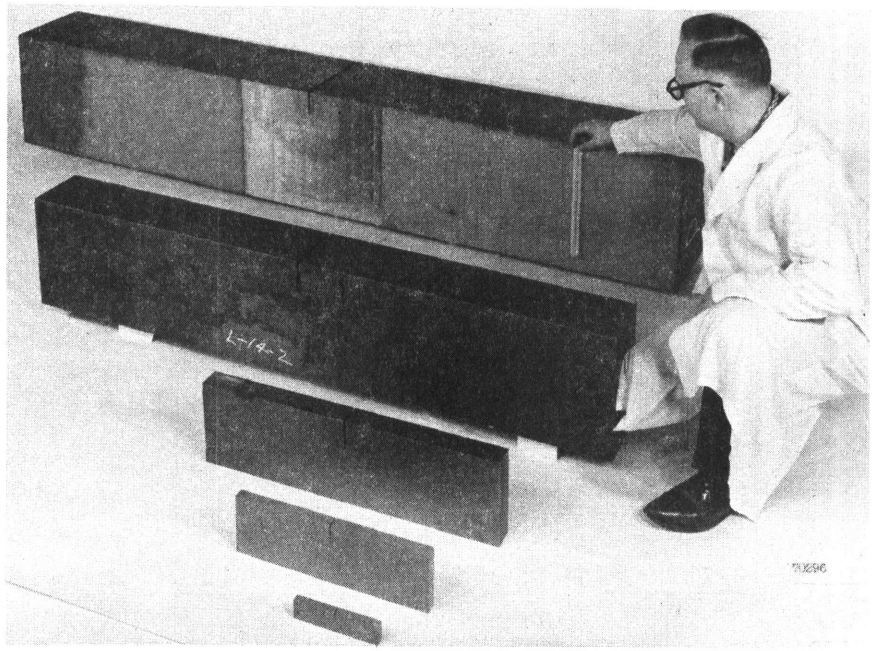

Fig. 5 - Various DT specimens in current use for size-effect studies ranging in thickness from 5/8 in. to 12 in.

Table 1
Dimensions and Weights of Various Steel Specimens Used in the DT Test

Specimen Designation	Thickness, B		Depth, W		Length, L		Span Between Supports, S		Brittle Weld or Notch Depth a		Weight	
	In.	Cm	In.	Cm	In.	Cm	In.	Cm	In.	Cm	Lb	Kg
5/8 in. DT*	0.625	1.6	1.62	4.1	7	18	6.5	16.5	0.5	1.3	2	0.9
1 in.	1	2.5	4.75	12.0	18	46	16	40.6	1.75	4.4	24	10
2 in.	2	5.0	8	20.3	28	71	26	66.0	3	7.6	127	57
3 in.	3	7.6	8	20.3	28	71	26	66.0	3	7.6	190	86
6 in.	6	15.2	12	30.5	62	158	58	147.3	3	7.6	1220	554
12 in.	12	30.5	15	38.1	90	228	84	213.3	3	7.6	4580	2080

*Also deep machined notch with tip sharpened by pressed knife edge.

Initial investigations were conducted on a 6-in. plate of A533-B Class 2 steel made to reactor-grade specifications. Mechanical properties and chemical analysis are presented in Table 2. The size-effect studies involved four thicknesses of DT specimens, ranging from 5/8 in. to 6 in. Figure 6 presents the data for 5/8-in. DT specimens involving through-thickness surveys for uniformity. The transition behavior is also reflected in the fracture surfaces, which are shown in the figure. Conventional DWT determinations of the NDT temperature at the 1/4, 1/2, and 3/4T positions indicate a range from 0 to 20°F. The indexing procedures define the limit of dynamic plane strain (end of regime 1) for the 5/8-in. thickness as approximately 45°F, the FTE as 65°F, and the FTP as 145°F. The specimens were taken in the RW (longitudinal) orientation.

Table 2
Chemical Analysis and Mechanical Properties for 6-in. A533-B Class 2 Steel

(a)
Chemical Analysis
Percentage

C	Mn	P	S	Si	Ni	Mo
0.23	1.18	0.007	0.014	0.20	0.57	0.46

(b)
Tensile Properties

Location	YS (ksi)	UTS (ksi)	Elongation (%)	RA (%)
Longitudinal				
Surface	79.3	99.2	23.8	66.6
1/2T	74.1	93.2	25.2	64.5
Transverse				
Surface	83.8	108.8	21.7	60.1
1/2 T	78.9	97.4	23.7	59.6

(c)
Charpy-V Data

Temperature (°C)	Charpy-V Values* (ft-lb)	
	Longitudinal (RW)	Transverse (WR)
-120	13	10
-80	25	18
-40	43	28
0	68	40
40	94	55
80	108	70
120	112	78
160	112	78

Note: Charpy-V energy at NDT (+10°F):* RW = 75 ft-lb and WR = 43 ft-lb
50% FATT:† RW = -15°F and WR = 0°F.
*Average for 1/4T and 1/2T locations.
†Fracture appearance transition temperature (50% shear).

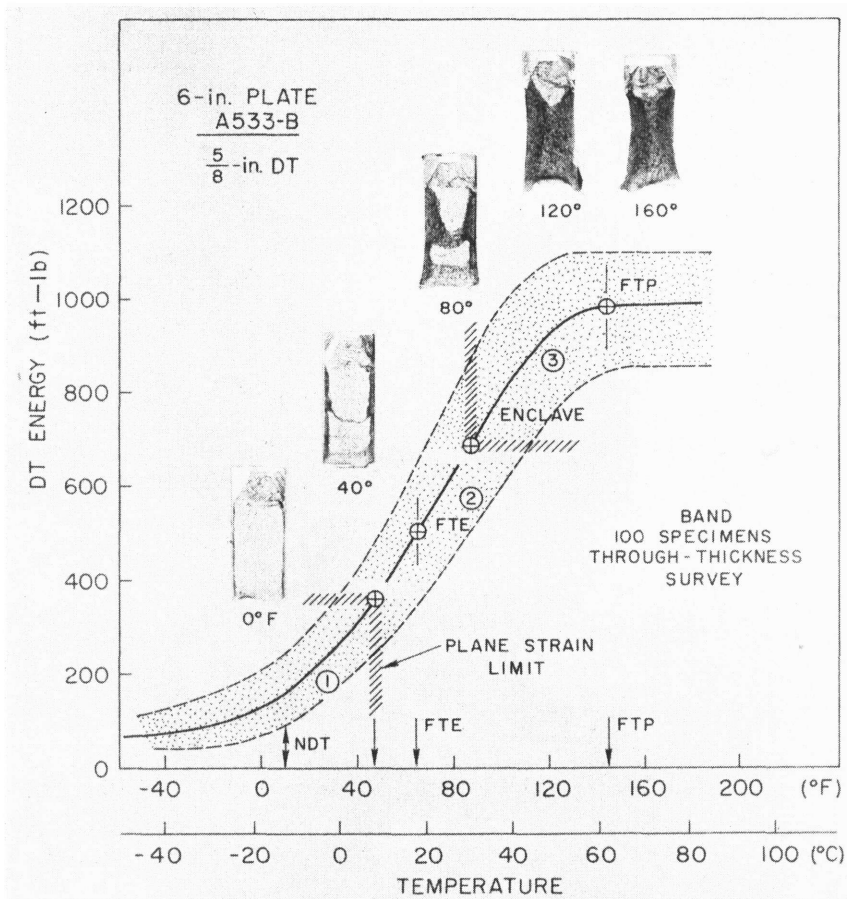

Fig. 6 - Procedure for indexing the 5/8-in. DT energy transition curve to the three characteristic regimes of fracture toughness transition. Data band for RW direction (longitudinal specimen) relate to through-thickness surveys of the 6-in.-thick A533-B steel.

A similar transition behavior is illustrated in Fig. 7 for the 3-in. (RW) and the full-thickness 6-in. (WR transverse) DT tests. The indexing procedures for the larger specimens define the limit of plane strain for both thicknesses as 125°F, the FTE as 140°F, and the FTP as 170°F.

Figure 8 presents a composite of the fracture surfaces for the 5/8-, 3-, and 6-in. DT specimens. The lines separate the fractures into the three regimes described previously. The changes in fracture appearance clearly reflect the increase in energy absorption and show a transition from flat fractures with small shear lips (regime 1), to fractures containing slight and then strong arrest markings (regime 2), and finally to fractures indicating large lateral contraction (enclave) and rapidly increasing areas of fibrous tearing (regime 3). The change in fracture appearance through DT regime 2 occurs dramatically in a narrow temperature range. The development of arrests is shifted to higher temperatures for thicker specimens, thereby indicating a size effect.

The magnitude of the size effect may be interpreted by normalizing the results of the various specimen sizes by the upper shelf energy or by the energy divided by the fracture area (E/A); the latter is chosen as a matter of convenience. The normalized

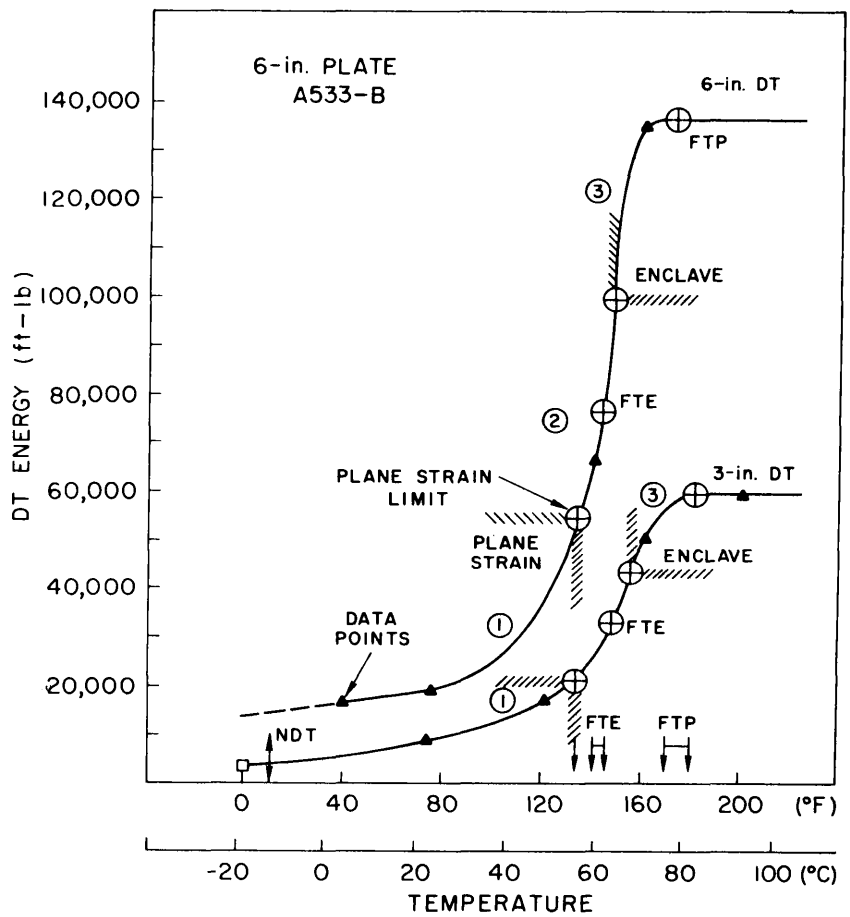

Fig. 7 - Results of 3-in. (RW) and 6-in. (WR or transverse specimen) DT test series for the 6-in. A533-B steel. The energy curves are indexed to the three characteristic regimes of fracture toughness transition.

E/A results for 5/8-, 1-, 3-, and 6-in. DT test sizes are presented in Fig. 9 for the 6-in. plate. Note that the curves for the thicker specimens are displaced to higher temperatures. If the 50% E/A points (FTE) are taken as a measure of the size effect, it is seen that the mechanical constraint imposed by the thicker sections results in a shift of approximately 70°F. The majority of the effect occurs between the 1-in. and 3-in. DT specimen sizes, with the 6-in. size showing negligible additional effects due to constraint. The constraint effect does not result in a uniform translation of the DT curve but occurs by an extension of regime 1. This result can be anticipated from fracture mechanics considerations since the thicker sections provide the mechanical constraint required to delay the transition to full ductility. However, the effects of constraint are not sufficient to suppress the transition to an arbitrarily high temperature; when the constraint is relaxed at higher temperatures, a rapid increase in microfracture ductility follows, which results in the highly ductile fractures shown for regime 3.

A similar series of DT tests was performed on a 12-in. plate of A533-B Class 1 steel as part of the HSST program. The plate properties are listed in Ref. 6. The plate has a tough surface layer that extends inward approximately 1.5 in. This is in contrast to the 6-in. plate, which has a tough surface layer of less than 0.5 in. The NDT temperature of the central region of the 12-in. plate was determined to be the same as the 6-in. plate;

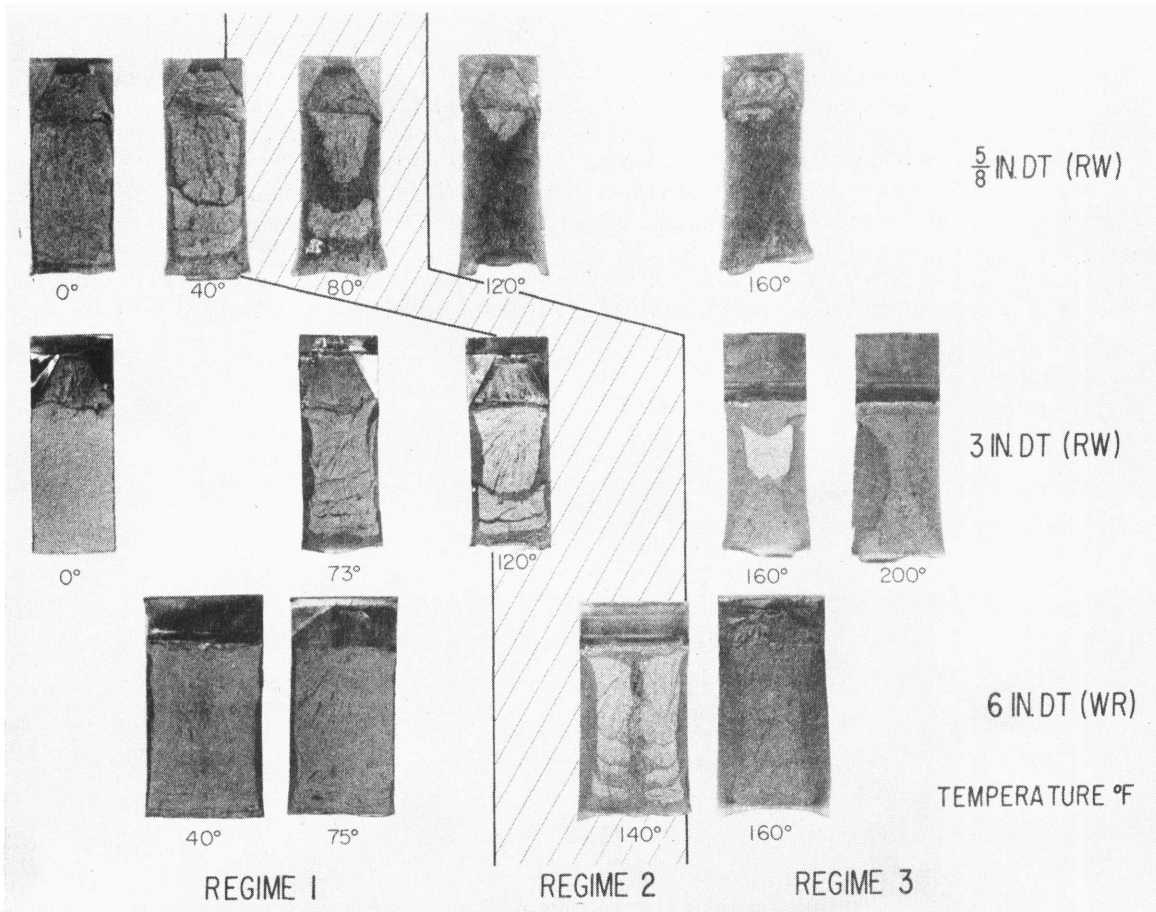

Fig. 8 - Correspondence of the fracture appearance transition of the DT test series to the three regimes defined by the energy transition curves in Figs. 6 and 7. Featureless, flat fractures of regime 1 are extended to higher temperatures by increased thickness. The arrest markings indicate transition through regime 2. Fibrous fracture and lateral contraction features indicate completion of the regime 3 transition.

thus, the data can be compared directly on the same temperature scale. The size-effect studies using 3- and 12-in. DT specimens (RW) indicate a corresponding transition from plane strain conditions to gross plastic deformation in generally the same temperature interval as 3- and 6-in. specimens from the 6-in. plate. However, the 750,000-ft-lb capacity of the large drop weight facility was insufficient to completely fracture a 12-in. DT specimen at the upper shelf temperature. Figure 10 shows the high degree of toughness exhibited by a 12-in. DT specimen tested at 215°F. The fracture extends approximately through two-thirds of the unbroken area and is characterized by a completely fibrous appearance. The huge lateral dimples (0.5 in. on each side) give evidence of the high fracture toughness. The E/A normalized data from the 5/8-, 1-, 3-, and 12-in. DT specimens are presented in Fig. 11. Since the 12-in. DT specimen tested at 215°F on the upper shelf was only partially fractured, the energy for a complete fracture is an extrapolation. The extrapolated value of 6400 ft-lb/in.^{2} was based on the shelf level trends exhibited by the smaller specimens (5/8 in. to 6 in.)

Figure 11 displays two sets of 3-in. DT data curves representing the surface layer and the midthickness material. These data illustrate the effect of the tough surface layer

in evolving the transition region for this material at a lower temperature than that for material from the midthickness location. As for the case of the 6-in. plate, it is seen that the major portion of the size effect occurs between the 1-in. and 3-in. thickness for DT specimens taken from comparable locations. The 1-in. DT curve illustrated for the 1/3T location applies to the 1/2T location as well. The E/A-normalized full-thickness, 12-in. DT points fall somewhat lower in temperature than the 3-in. DT curve for the 1/2T location but not as low as the 3-in. DT surface material. This reinforces the observation that relatively little size effect is developed above the 3-in. DT sizes and leads to the conclusion that the shift noted for the 12-in. DT test (i.e., slightly to the left of the 3-in. DT curve for 1/2T) is a result of the tough surface material. The size effect at the 50% E/A point is approximately 50° F, which compares favorably with the deduction for the 6-in. plate.

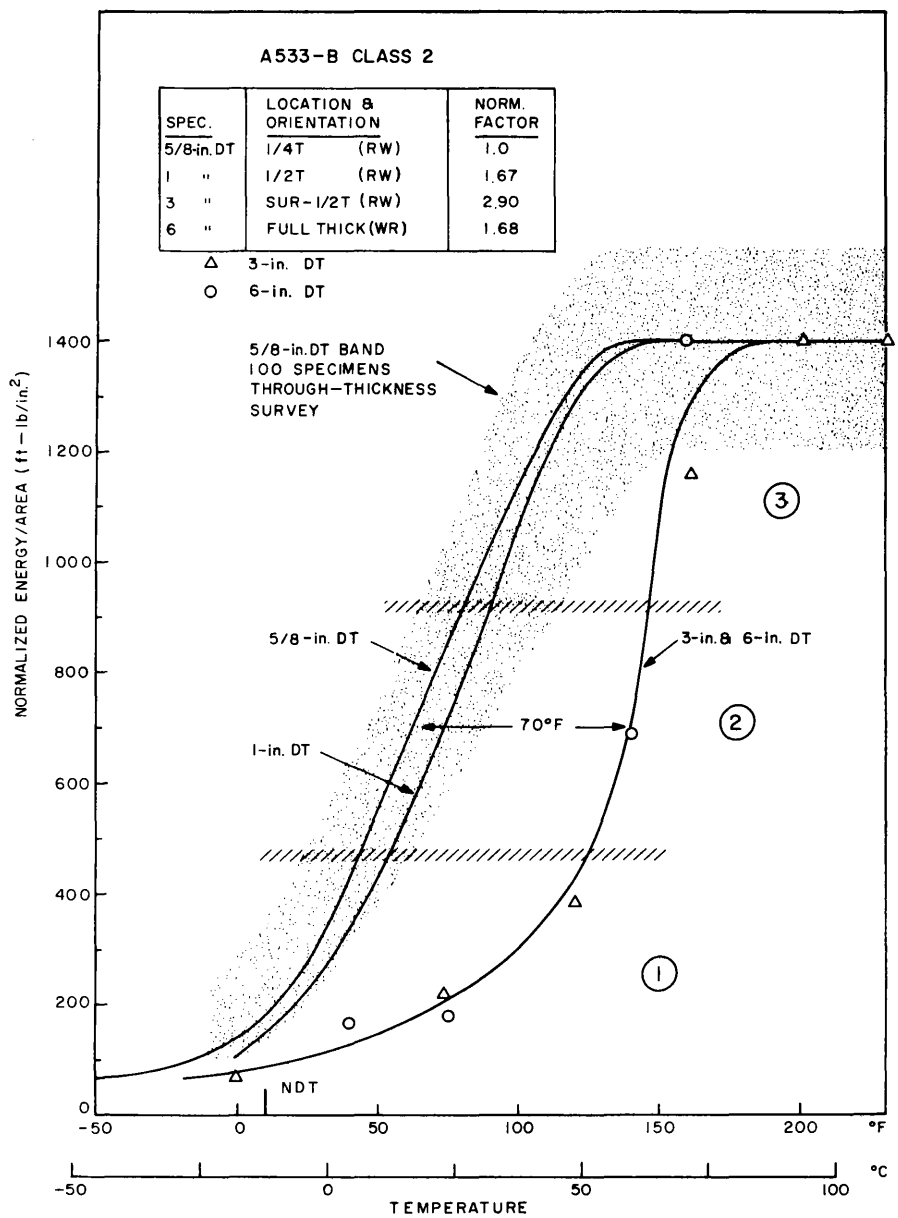

Fig. 9 - DT test curves for various thickness specimens which are normalized on the basis of upper shelf energy/fracture area. The normalization procedure indicates a size effect on the order of 70°F for the 6-in. A533 steel.

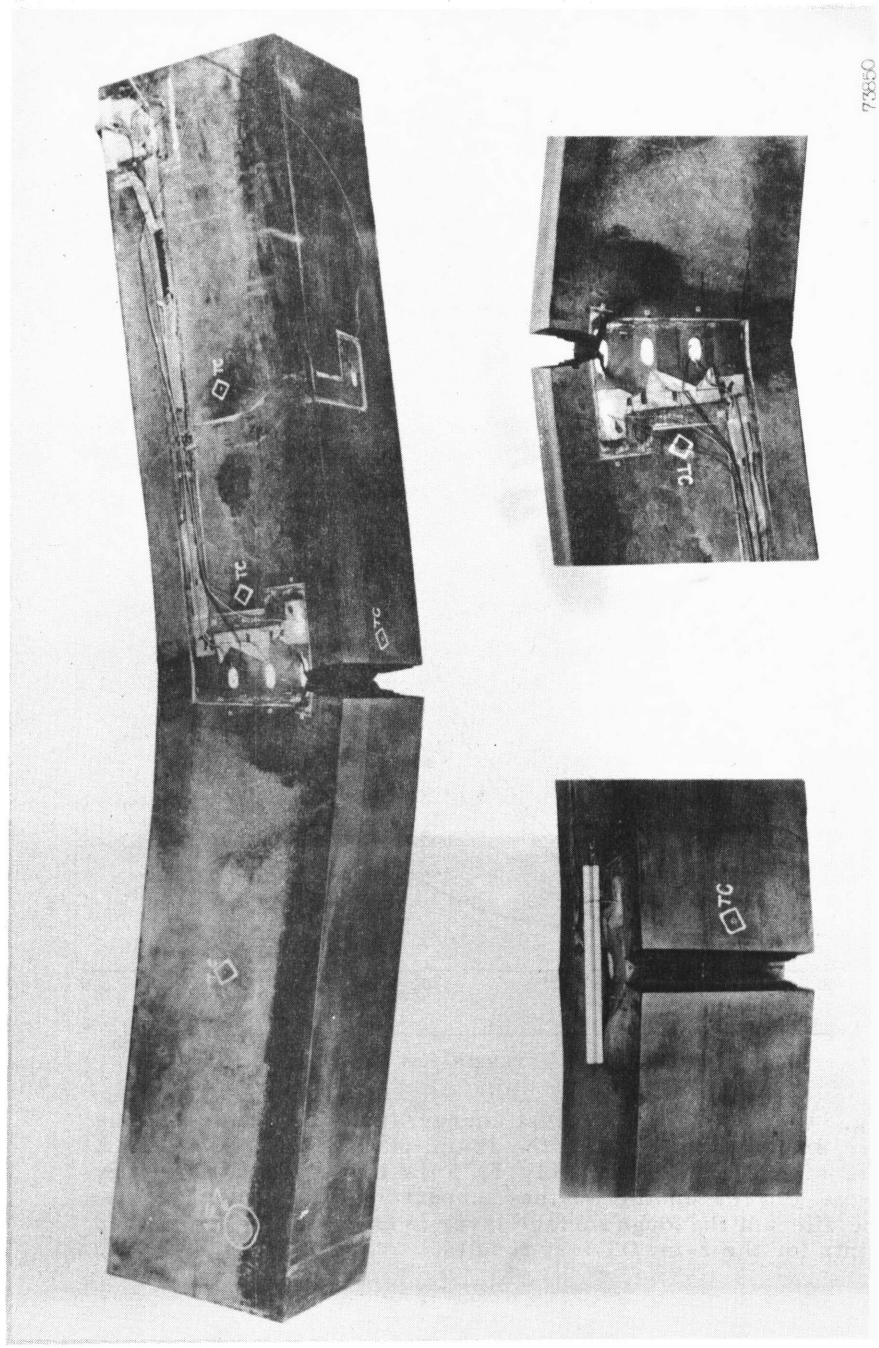

Fig. 10 - Illustration of the 12-in. DT test specimen of A533-B steel, which exceeded the capacity of the 750,000-ft-lb drop-weight testing machine at the upper shelf temperature of 215°F. A high degree of fracture toughness is indicated by the lateral dimpling (0.5 in. on each side).

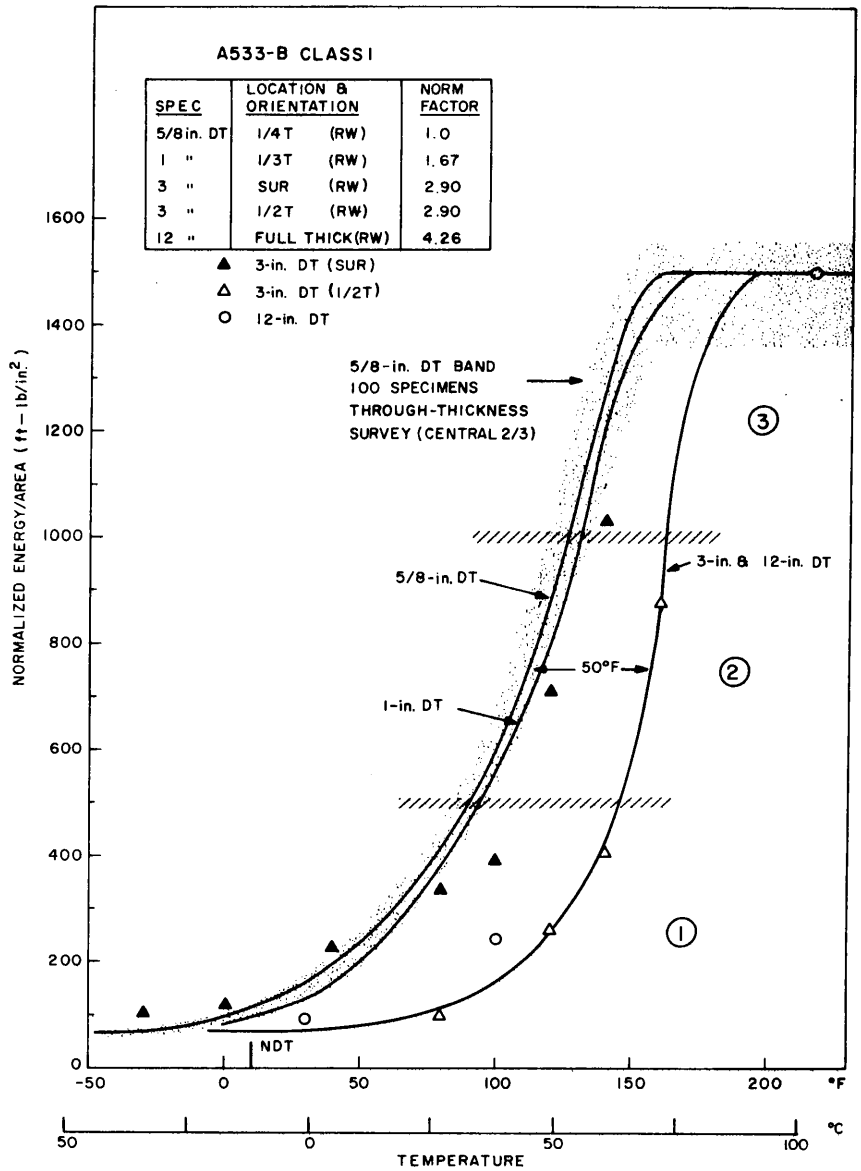

Fig. 11 - Normalized DT test energy/area curves for various size specimens cut from the 12-in. plate of A533-B steel. A size effect of approximately 50°F is indicated at the energy levels corresponding to the respective FTE temperatures. The effect of the tough surface layer is indicated by the shaded points for the 3-in. DT test results.

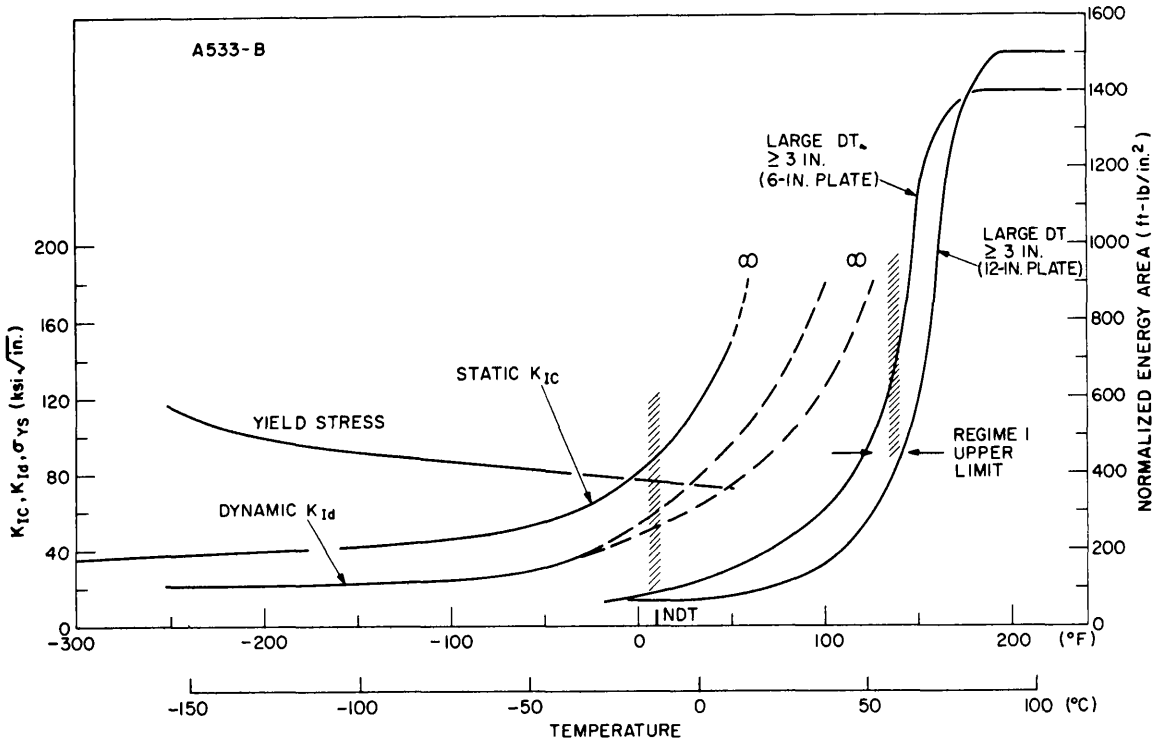

Fig. 12 - Comparison of thick-section DT test results with static K_{Ic} and dynamic K_{Id} data for A533-B steel. Large-section (12-in.-thick) K_{Ic} specimens did not extend the measurement capacity of static plane strain fracture toughness beyond NDT + 40°F. K_{Id} values are extrapolated to higher temperatures, but it is evident from the sharply rising region of the thick-section DT tests, that K_{Id} specimens of large size would not extend the measurement capability beyond the limit defined by the DT tests.

COMPARISON OF FRACTURE MECHANICS AND DT TESTS

The size-effect studies are highly significant in that they show a transition temperature behavior for very thick specimens that is similar to that displayed by the small specimens. The distinguishing feature of the thick-section material is an extension of regime 1 of the transition and a shift of the FTE temperature on the order of 60°F resulting from increased mechanical constraint. It may be concluded that the increase in microfracture ductility is a fundamental process which determines the existence of a temperature-induced transition regardless of test procedures. Accordingly, large-size K_{Ic} and K_{Id} tests must likewise project a fracture toughness transition which terminates to infinity limits below the LTTR defined by the DT test.

Westinghouse Research Laboratories investigators have completed the large-size K_{Ic} tests which are required to resolve the constraint effects issue as related to fracture mechanics parameters. This investigation was conducted in conjunction with the previously described HSST program (7). The K_{Ic} results of compact tension specimens (CTS) including the full thickness of the 12-in. plate of A533-B (HSST plate 02) steel are presented in Fig. 12 and compared with the DT test data. The K_{Ic} data clearly indicate a dramatic transition temperature increase, which begins in the vicinity of the NDT temperature. Valid K_{Ic} numbers were not obtained at temperatures higher than 50°F (i.e., NDT + 30 to 40°F) at which point a K_{Ic}/σ_{ys} ratio of 2.0 was measured, requiring a 12-in.-thick specimen. The infinity (∞) notation on the K_{Ic} curve signifies a projection to infinitely high ratios within a small temperature increment. In effect, this denotes

the highest temperature to which static linear elastic fracture mechanics (LEFM) is applicable for this steel. For specimens of less than 12-in. thickness, the limit for valid K_{Ic} measurements must occur at lower temperatures, as shown schematically in Fig. 2.

Figure 12 also illustrates the thick-section DT test behavior for the 6-in. and 12-in. A533-B plates presented in Figs. 9 and 11. The small temperature displacement of the DT curves for the two plates (less than 20°F) is within the limits of reproducibility of the data and is not interpreted to represent a size effect between 6-in. and 12-in. thicknesses. It was stated previously that the upper bound of regime 1 for the DT test defines a temperature above which LEFM is not applicable. The static K_{Ic} results in Fig. 12 obviously bear out this fact, since the static K_{Ic} temperature limit is approximately 75°F below the limit defined by regime 1. The reason for this temperature difference is that the DT test involves dynamic fracture and is therefore taken to represent a conservative upper bound for dynamic K_{Id} tests. The latter tests should enable dynamic LEFM to be extended to higher temperatures than for the static case. Unfortunately, heavy-section K_{Id} data for A533-B steel do not exist on which to verify this conclusion.

A limited amount of K_{Id} data are available (4,8,9) for A302-B steel and are presented in Fig. 12. The A302-B steel used for the tests is the precursor of A533-B. The particular heats involved featured a similar NDT (0 to 20°F) as the described 6- and 12-in.-thick A533-B steels. The A302-B composition is similar to that of the A533-B, with the exception of 0.6% nickel in the latter. The K_{Id} data are assumed to be a fair representation of the expected behavior for A533-B. The data extend from very low to approximately the NDT temperature and were obtained using specimens of 5/8-in. and 1-in. thickness and loading rates of 10^4 ksi $\sqrt{\text{in.}}$/sec. The K_{Id} values are approximately 60% of the K_{Ic} level at a given temperature. A projection of K_{Id} values is made to higher temperatures using the existing data and the premise that valid K_{Id} data cannot be obtained above regime 1 of the DT curve. The performance of the DT test above regime 1 provides clear evidence that dynamic LEFM is inapplicable above this temperature range because the fractures are of the ductile type.

Large-section K_{Ic}, K_{Id}, and DT testing is very expensive and cannot be performed routinely for purposes of engineering characterization. It is inescapable that the performance of small specimen tests must be used to interpret the fracture characteristics of large sections. This can be done based on 5/8-in. DT specimen data and then adding a temperature increment to account for the size effect, as follows. Since the large-section-size DT test curve rises very steeply in regime 2, there is little difference between the end of regime 1, signifying the limit of LEFM applicability, and the FTE defined by the energy midpoint. As a matter of convenience the thick-section FTE can be taken as an index of the limit of plane strain applicability. The thick-section FTE can be indexed by a size effect of 60°F added to the FTE determined with a small-size DT specimen. In this manner it is possible to define a temperature region above which LEFM calculations are not applicable because of the resulting infinitely high dynamic ratios of K_{Id}/σ_{yd}.

The conservatism of the above approach requires that better and possibly more expensive steels may have to be used to lower the FTE temperature of thick sections to operating temperatures. If it is not desired to pay this premium, it is necessary to use a calculative technique, such as LEFM, which requires an exact knowledge of the existing flaws and their associated stress fields. The LEFM technique is generally applicable up to the NDT temperature using small-size test specimens. However, a temperature span of approximately 120 to 140°F can exist between the NDT and FTE for which K_{Id} data do not exist and K_{Ic} calculations cannot be made, even if desired. Figure 12 shows that thick-section K_{Ic} tests will provide only an additional 40°F of "calculation regime"

above NDT. The routine development of K_{Id} data to extend dynamic LEFM to higher temperatures entails serious experimental difficulties, yet unresolved. The only practical solution which can be considered presently for the regime between NDT and FTE is correlative approaches. One such approach is to use the extrapolated ratios of K_{Id}/σ_{yd}, based on the DT results, for the calculation of flaw size-stress relationships from LEFM formulas. An alternative approach is to use the FAD as modified recently to include section size effects (10). The modified FAD is discussed in a subsequent section.

Further comments are in order concerning the applicability of static, as opposed to dynamic, fracture mechanics parameters. Concern has arisen in the field of fracture mechanics relative to the experimental determination of K_{Ic} values and with respect to whether the static value for fracture instability can be relied on generally for the case of loading rate sensitive steels of relatively low strength. The problem is that the experimental procedures for the measurement of the static K_{Ic} values depend on events involved with very small, initial, slow extension of the crack (creeping instability) prior to attaining a fast fracture. Some steels appear to tolerate more of this gradual "creeping" extension of the crack of microscopic dimensions than others. It appears that this type of crack extension should be developed to a greater degree with increasing temperature, i.e., as a consequence of a sharp rise of K_{Ic} values with increased temperature.

In brief, the K_{Ic} determination may become controlled by complex events involved in creeping, slow extensions of the crack rather than by a clear-cut popin instability. Thus, there is a question as to the reliability of using K_{Ic} values based on such events as the basic criteria for fracture-safe design. It is suspected that such events may be critically related to small differences in loading rate and as such would suggest placing increased emphasis on K_{Id} rather than K_{Ic} values for fracture-safe design. For example, if the K_{Ic} value is controlled by the initial slow extension of the crack, there is no guarantee that test results will be duplicated in a structure. Moreover, the possibility of developing embrittled regions at the tips of natural cracks would dictate that the dynamic fracture considerations must be emphasized in determining fracture safety.

FRACTURE MECHANICS INTERPRETATIONS OF NDT

The remainder of this report is addressed to a further analysis of existing transition temperature approaches to fracture-safe design, namely, NDT and the FAD. This section deals with the significance of the Drop Weight-NDT in terms of the temperature dependence of critical flaw sizes. The NDT as defined by ASTM standard E-208-66T signifies the upper temperature limit for dynamic fracture initiation from small flaws subjected to yield stress loading. The size of the flaw was designated to be of arc-strike or weld-defects proportions. The low strength steels, for which this method was originally used, exhibit a sharp increase in dynamic fracture toughness above the NDT to the extent that flaws of relatively large size would require plastic overloads for fracture initiation at NDT + 60°F. This behavior is the basis for the DWT-FAD interpretative procedure. In approximately 15 years since the DWT was introduced to general engineering use, research questions concerning the test have arisen in relation to the newer types of steels and size effects associated with thick sections. Most of these questions can be resolved through fracture mechanics analyses of the DWT and by results of tests involving thick sections.

Irwin (11) has analyzed the DWT test in terms of fracture mechanics aspects. The brittle weld is taken to represent a 1:4 (depth-to-width aspect ratio) surface flaw dynamically loaded to yield stress levels. Using a crack depth of 0.2 in., a ratio of K_{Id}/σ_{yd} can be calculated from Irwin's equation for a semielliptic flaw in tension:

$$K_{Id}/\sigma_{yd} = 1.1\sqrt{\frac{\pi a}{Q}}$$

where a = crack depth (in.)

Q = flaw shape factor (tabulated)

σ_{yd} = dynamic yield stress (ksi)

The above calculation gives a ratio of $K_{Id}/\sigma_{yd} = 0.78$. The actual DWT flaw geometry varies between a 1:4 and 1:3 aspect ratio. Using the latter ratio gives $K_{Id}/\sigma_{yd} = 0.71$.

The following formula of Smith (12) for a surface flaw in bending more nearly duplicates the loading condition of the DWT test and is considered to be a more definitive equation to use for this calculation:

$$\frac{K_{Id}}{\sigma_{yd}} = M_b \frac{\sigma}{\sigma_{yd}} \sqrt{\frac{\pi a}{Q}}$$

where σ = bending stress (ksi)

M_b = flaw constraint factor (tabulated)

Since the equation will be used for the case of yield stress loading in the region of the flaw tip, the factor σ/σ_{yd} becomes unity. The only difference between the Irwin and Smith formulas is the factor before the radical. The factor M_b depends on the ratio of flaw depth to specimen thickness and approaches Irwin's 1.1 for very large thicknesses. Applying Smith's equation for the standard DWT specimen thickness of 5/8 to 1 in., and using flaw aspect ratios of 1:3 and 1:4, gives values for the ratio of K_{Id}/σ_{yd} that vary from 0.4 to 0.6. A mean value of $K_{Id}/\sigma_{yd} = 0.5$ is taken as a representative fracture mechanics interpretation of the DWT dynamic fracture toughness measurement capability. Any finer definition is believed to be impractical. Recent investigations by Shoemaker and Rolfe (9) based on K_{Id} studies for steels ranging from 35- to 135-ksi yield stress (including A302-B) show a measured $K_{Id}/\sigma_{yd} = 0.6$ as an upper bound at the NDT temperature. These data present experimental verification of the theoretical determination that the NDT temperature refers very closely to a ratio of $K_{Id}/\sigma_{yd} = 0.5$.

When the DWT is considered in the above fracture mechanics framework, it can be seen that the ratio $K_{Id}/\sigma_{yd} = 0.5$ properly fits the dynamic K_{Id} curve of Fig. 12. Cognizance must be taken of the fact that, according to Irwin (11), the dynamic yield stress is elevated by about 25 to 30 ksi over the static yield stress shown in Fig. 12. This ratio value denotes fracture toughness conditions where flaws on the order of tenths of inches deep are critical for yield stress levels of loading. The K_{Id} curve rises rapidly with temperature; therefore, the critical flaw sizes must increase correspondingly. The ratio K_{Id}/σ_{yd} and resulting critical flaw sizes would reach very large proportions in the 60°F interval above the NDT temperature. The rapid upsweep in dynamic fracture toughness is the reason why the transition temperature approach of NDT + 60°F guarantees structural safety for large flaws at yield stress loading, within a small temperature increment above NDT.

From the data presented herein it becomes apparent that section size does not play a role in the interpretation of the significance of the NDT temperature. This point has created questions in relation to the DWT for many years, since it was assumed by some that the NDT temperature would be shifted to higher temperatures for thick sections; this is incorrect. The NDT value is not dependent on thickness, because a 5/8-in. DWT specimen provides sufficient plane strain constraint for the specified flaw size at the NDT temperature. Therefore, thick specimens cannot provide additional constraint to lower the dynamic K_{Id} value measured by the standard DWT specimens.

The thickness question was investigated by Puzak and Babecki in the late 1950's (13). This investigation showed that the NDT temperature is invariant with thickness for test specimens of 5/8-in. to over 7-in. thickness using various structural steels and the same size weld bead. The confusing aspects which have arisen in other studies are that an apparent NDT temperature shift will occur if the weld crack-starter flaw is scaled up with thickness or increased bending strain is imposed. The effect due to increased size of weld bead is obvious from the temperature-dependence aspects of the K_{Id} curve. A larger flaw would remain critical (for yield stress loading) to a higher temperature, since a higher applied K level is imposed. The temperature defined by the DWT-NDT denotes a fundamental transition in microfracture ductility, which is of major engineering significance and provides for the use of a practical test of utmost simplicity for its determination.

The answer to the question of thickness effects lies in the fact that the K_{Id} curve will not rise as sharply for thick specimens as it does for thin specimens; this is indicated by the thin and thick section DT test data of Figs. 9 and 11. The practical implication of this phenomena is that NDT + 60°F does not guarantee the same degree of safety for thick sections containing large flaws as it does for thin sections. In actuality, this means that there is a shift in the FTE for thick sections, since a size effect on the order of 60°F must be added to the NDT + 60°F definition of FTE as measured by thin sections. This fact is recognized, and it has been used to modify the FAD to include both thin and thick sections, as presented in the following section.

THICKNESS EFFECTS INTERPRETATIONS OF THE FAD

The FAD represents a practical procedure for the synthesis of fracture mechanics and transition temperature concepts. As originally developed (3) this diagram was validated by failure analyses for the transition region between the NDT and FTE temperatures based on relatively thin sections. This procedure has now been expanded to include thick sections. Both the original and expanded versions are presented in Fig. 13. The method continues to introduce experience into the analysis through correlation with service failures. The flaw sizes defined by the FAD were derived from service experience and later verified by fracture mechanics flaw size calculations (2).

The important aspect of the FAD is its definition of the effects of increased temperature above the NDT on flaw size-stress relationships. It is the grouping of flaw sizes into discrete ranges (i.e., small, medium, large, and very large) that makes such definitions feasible, and also practical, for engineering use. The flatness of the flaw size curves at the NDT temperature is not meant to imply the absence of temperature effects below this temperature but only that this is the starting point of the diagram. This fact is indicated by the absence of a temperature scale below NDT. Accurate flaw size-stress relationships below NDT are obtainable through the use of LEFM. On the other extreme, the FAD extrapolates into the plastic stress region. These extrapolations serve only to indicate that the plastic stress level required for fracture should increase with temperature. The plastic stress levels are not indexed, because there are no methods of calculations or failure experience which would indicate specific relationships. Since structures are not normally designed for plastic loading, the prime interest is in the elastic stress region of the FAD.

Fracture mechanics flaw size calculations for the NDT temperature have brought to light the fact that all but the smallest flaws (less than 1 in.) must relate to static initiation. Knowing the dynamic ratio $K_{Id}/\sigma_{yd} = 0.5$ at NDT enables calculations to be made for critical flaws at all levels of stress. However, the known service failures have involved larger flaws than those calculated dynamically, thereby implying static initiation conditions. Only the small flaws correspond to conditions of dynamic initiation. This

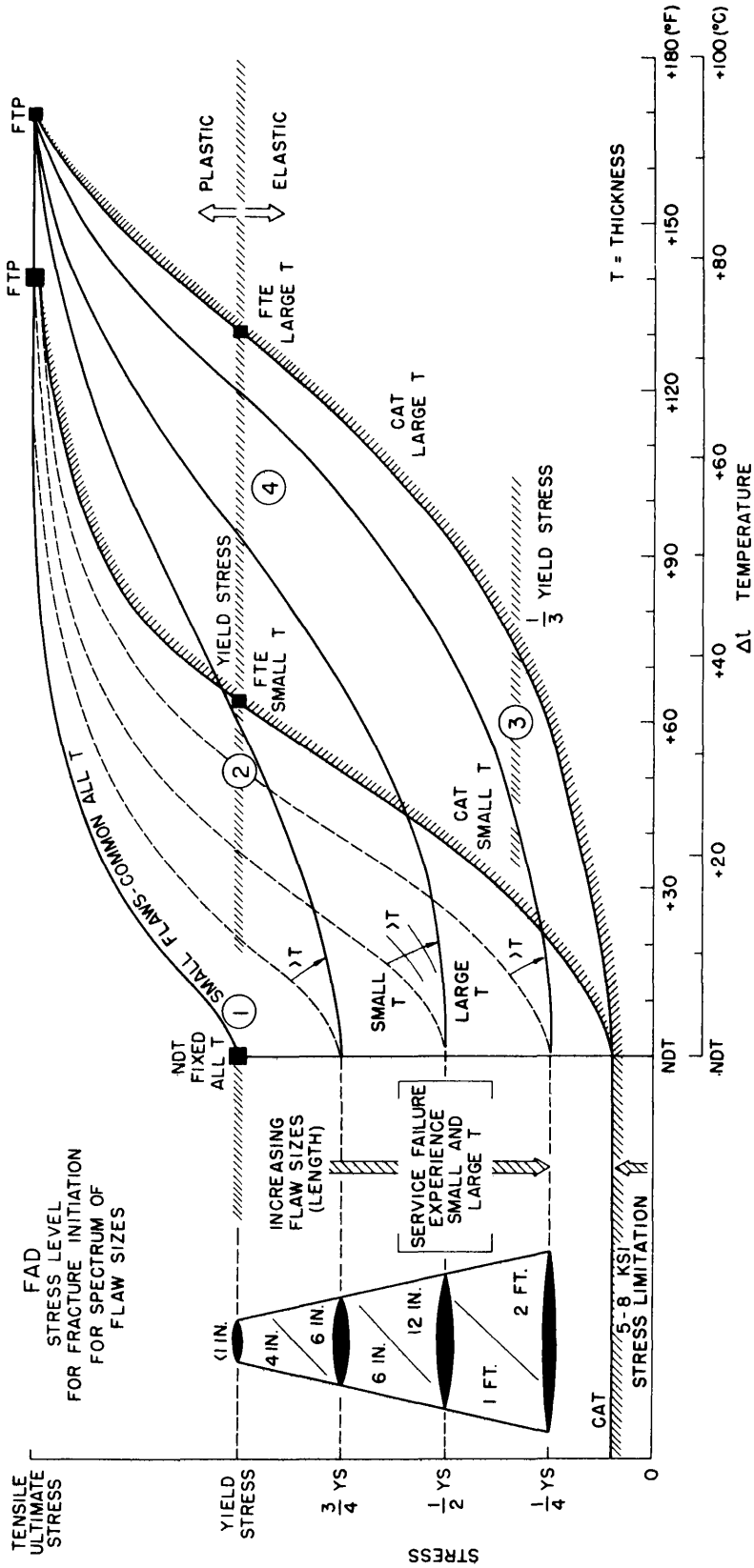

Fig. 13 - FAD for flaws residing in sections of small and large thickness

observation explains the spread in the flaw size curves of the FAD. It is expected that the various curves would be shifted closer to the CAT if the flaws were dynamically initiated. The flaw size-stress level curves of the FAD reflect the fact that higher stress levels are required for static conditions than are required for dynamic K_{Ic} conditions.

Size effects due to thick-section constraint require an expansion of the original FAD. This is accomplished by setting the upper temperature boundary as the thick-section CAT curve corresponding to definitions of thick-section DT tests. This follows from the fact that mechanical constraint imposed by thick sections enables plane strain conditions to be attained to higher temperatures and delays the transition to plastic fracture conditions. The upper bound curve, corresponding to flaws less than 1 in., cannot be altered significantly by mechanical constraint, because plane strain conditions already exist at the NDT temperature for thin sections. The only effect section size can have on the small flaw curve is in the plastic region. Since the curve in that region is extrapolated, it will be assumed that it is essentially invariant with thickness. The thick-section CAT curve and the small flaw curve establish envelope limits for the case of thick sections. The maximum shift in the CAT curve due to thickness occurs at the level of yield stress loading, for which case it is on the order of 60°F. The remaining flaw size curves are proportioned in the envelope based on the K_{Ic}/σ_{ys} temperature-dependence extrapolation to NDT + 60°F, as shown in Fig. 13. The effects of section size would be expected to lower the dashed curves for thin sections (labeled as small T) as indicated in the figure.

The FAD expansion due to thick-section constraint is illustrated by four examples corresponding to the numbers coded in Fig. 13.

Case 1 - This condition refers to small flaws in regions of geometric stress concentration or high residual stress, such as in weld heat affected zones. Thick sections will not result in shifts of this condition for reasons already brought out.

Case 2 - This condition can be taken to represent flaws in the order of 6 in., located in regions featuring near yield stress loading, such as a nozzle of a large pressure vessel. The shift due to section size for the case of static initiation is approximately 40°F. If the flaw was dynamically loaded, an additional temperature increment of 40 to 60°F would have to be added to place this condition near the thick-section CAT curve.

Case 3 - Very large flaws are required for static instability at levels of stress on the order of 0.3 yield stress, even at the NDT temperature. Thick-section constraint is expected to elevate this condition approximately 50°F. The addition of dynamic loading is expected to have little additional effect because of the proximity of the CAT curve.

Case 4 - This condition relates to the unusual case of a large flaw residing in a region of yield stress loading and would have a section size shift of approximately 60°F. This estimate is highly conservative, because it assumes extrapolation of K_{Ic}/σ_{ys} to NDT + 100°F, whereas it actually terminates at NDT + 40 to 50°F. Again, dynamic initiation is expected to have little additional effect.

In consideration of the above cases, it is apparent that the 60°F size effect determined from the DT test cannot be directly translated to similar shifts of all FAD flaw curves of the original diagram. The most common failure conditions of very small flaws located in highly stressed regions of geometric transition are not affected significantly by large increases in section size. Statically loaded flaws located in large sections can undergo shifts due to section size, which do not exceed 60°F as based on the original FAD definition. Dynamic loading may be expected to increase the shift to the limits defined by the CAT curve for the thick sections.

FAD APPLICATION TO PRESSURE VESSELS INVOLVING GEOMETRIC INSTABILITY

Apparent discrepancies in the use of the FAD have arisen from the fact that fractures of pressure vessels may be initiated and propagated at nominal hoop stress levels above the CAT or FTP temperatures. This condition is possible only for the case of flaws which are very long with respect to the wall thickness. This fact was reported and explained in the original publication (3) of the FAD. Such failures are due to geometric instabilities (GI) leading to bulging of the metal around the flaw, resulting from plastic overload. The term geometric instability relates to the fact that such flaw lengths in the subject vessels create a large unsupported region. The resultant bending force, caused by very low elastic stresses, is sufficient to overload the unsupported metal and cause failure. This situation was brought out in the original data of 1-in. burst vessels featuring two sizes of flaws 10 in. (10T) and 20 in. (20T). These data are plotted in Fig. 14 and indicate failure stress curves which rise only gradually above the nominal hoop stress failure levels indicated for the NDT region.

It should be obvious that, when flaws become so large as to cause geometric instabilities, no degree of metallurgical toughness is sufficient to preclude failure. This behavior can be compared to the buckling of a column for which failure depends on only the geometry and modulus, once the critical load is attained. Failures will be equally dramatic for materials of low and high fracture toughness. Consequently, it is not correct to use a fracture mechanics approach, or any other approach based on fracture toughness, to analyze this behavior. Therefore, it cannot be stipulated that the failures shown in Fig. 14 invalidate the FAD. On the contrary, the toughness transition is still displayed for the failures of Fig. 14 as was illustrated in Ref. 3. The fractures below the NDT temperature showed a brittle condition, while those above the CAT indicated a high degree of bulging associated with large energy absorption. Fortunately, the flaws of 10T and 20T proportion necessary to cause geometric instability are unrealistically large for thick sections, where they would refer to flaw lengths on the order of meters.

Two additional factors must be brought out with respect to geometric instability failures - one relates to the extent of fracture and the other relates to the stress level to be used in indexing the failure. Discussion presented in Ref. 3 emphasized that the pneumatically loaded vessels feature much more drastic failures than the hydraulically loaded vessels. The reason for this becomes apparent when it is realized that the driving force in the hydraulically loaded vessel soon dissipates as the crack opens up, while the force associated with the pneumatically loaded vessel can remain undiminished for longer time periods as the gas expands and therefore causes more extensive damage.

It must be remembered that the proper stress level required for entering the FAD analysis system is the local stress field in which the flaw resides. If this stress field is elevated to above yield levels by the large plastically deformed area due to the bulging which precedes a geometric instability failure, the correct stress to use is yield or tensile ultimate and certainly not the elastic hoop stress. The failure conditions noted in Fig. 14 are plotted as a function of hoop stress to illustrate the relationships between flat plate loading and geometric instability loading. The stress level actually experienced by the flaw tip region is approximately that of the flat plate case, which is basic to the FAD definition of failure conditions. It is emphasized also that no basic analytical method, including fracture mechanics, would provide for direct calculations based on hoop stress for cases of geometric instability. Calculative methods do not exist for cases involving. fracture by ductile processes. Recourse must then be made to the evaluation of such conditions by empirical approaches based on experimental data. However, these cannot be translated from thin to thick sections; large-section size failure tests must be conducted.

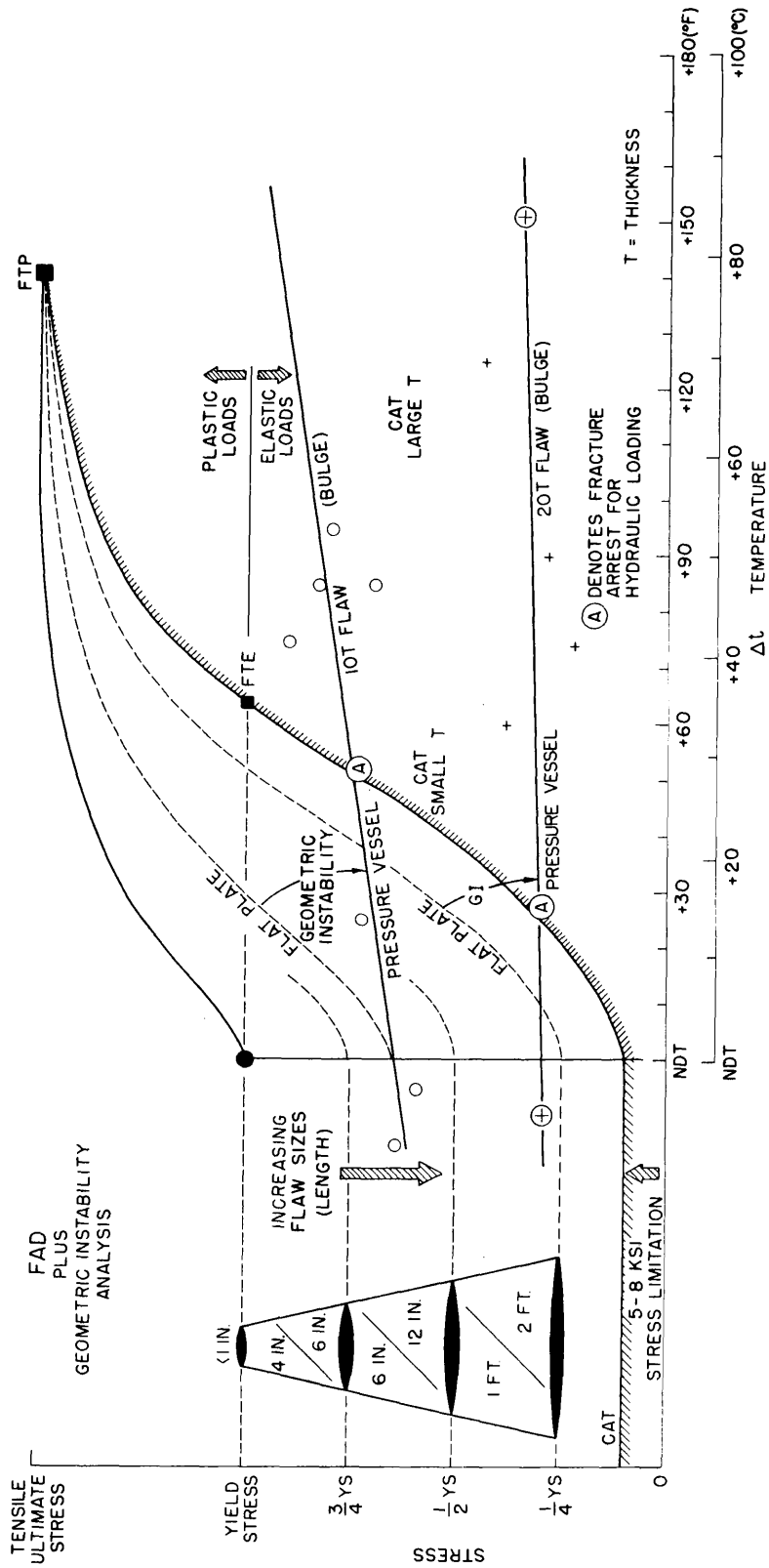

Fig. 14 - Extension of FAD to include conditions of geometric instability (bulging) for thin-walled (1-in.) pressure vessels containing long flaws in relation to the wall thickness. These relationships cannot be applied directly to thick-walled vessels by the use of FAD or any other procedure.

SUMMARY

The effect of mechanical constraint imposed by thick sections has been examined in the framework of linear elastic fracture mechanics and transition temperature approaches to failure analysis. Theoretical predictions of fracture mechanics have lead to the belief that thick-section steels, of shelf toughness and strength classes similar to A533-B, will not exhibit a transition temperature behavior. The consequent prediction for brittle behavior at temperatures on the order to 300 to 400°F above the NDT temperatures caused serious concern over the operation of thick-section structures, particularly reactor pressure vessels. These theoretical considerations have been shown to be in error through interpretation of thick-section fracture mechanics and Dynamic Tear (DT) tests. Thick-section A533-B steels exhibit a transition behavior similar to that of thin sections. The major distinguishing feature of the thick sections is a size effect involving an extension of regime 1 of the transition and a shift of the FTE temperature on the order of 60°F.

Fracture mechanics correctly predicts that increased mechanical constraint should inhibit the increase of crack tip ductility with increasing temperature. However, mechanical constraint has finite limits which can be effective only in the initial stages of increased microfracture ductility with increased temperature. Beyond a limiting temperature the microfracture ductility becomes too high, and mechanical constraint is lost. This behavior leads to the concept of a limiting transition temperature range (LTTR). The DT test of thick-section specimens is considered to define the true LTTR.

The DT test transition curve can be divided into three regimes. These regimes are shown to indicate similar fracture transition features for specimens of thickness ranging from 5/8 in. to 12 in. Regime 1 defines a zone through which fracture mechanics (both static and dynamic) becomes inapplicable with small increases in temperature. This regime is also shown to correspond to the temperature range of the Robertson Crack Arrest Temperature (CAT) curve. Regime 3 is shown to represent fractures exhibiting large plastic deformation for which suitable fracture mechanics analyses have not been developed. Regime 2 defines a transition between the two extreme cases; the midpoint energy, located in this regime, is defined as the FTE. The size-effect studies conducted with the DT test indicate that the thickness-controlled shift of the FTE appears to saturate for thicknesses in excess of 3 in.

It is recommended that steels which provide for service at temperatures above FTE should be selected whenever practical because of the enormous increase in fracture toughness in a small temperature interval through the FTE temperature region. Such selection will obviate the need for refined size-stress level calculations. If the above approach cannot be followed, critical flaw size calculations must be made. Unfortunately, the 120 to 130°F temperature interval between NDT and the thick-section FTE does not presently lend itself to fracture mechanics computations. Expensive thick-section K_{Ic} tests will only extend the measurement capability for a fraction of this temperature interval. Dynamic K_{Id} tests are preferable to K_{Ic} tests in view of the uncertainty in measurement of static flaw tip instability conditions. In any event, the static initiation always leads to dynamic propagation; i.e., the engineering consequences are always related to conditions of dynamic fracture. Unfortunately, no K_{Id} values exist for the temperature region above NDT. Specimens of large dimensions are required, and the experimental determination of the K_{Id} value is presently a research undertaking. The only practical alternatives to this problem are to use extrapolated K_{Id}/σ_{yd} ratios based on thick-section DT tests or to use the Fracture Analysis Diagram (FAD), as extended to include thick sections. The latter is preferable in view of the service experience which it incorporates.

The DWT-NDT and FAD interpretation procedures have now been analyzed in terms of fracture mechanics. The NDT is shown to correspond to a K_{Id}/σ_{yd} ratio of 0.5.

Questions concerning size effects for this test have been clarified. The NDT is invariant with thickness as long as the original flaw size is retained. The applicability and engineering value of the FAD rests on the sharp upsweep of K_{Ic}/σ_{ys} and K_{Id}/σ_{yd} ratios in a limited temperature increment above NDT. This basic metallurgical characteristic leads to a rapid increase in critical flaw size, as verified by fracture mechanics tests and calculations.

The transition temperature approach is useful only for steels exhibiting a transition to high shelf fracture toughness, such as described in the text. For steels involving very low values of shelf toughness, flaw size-stress level calculations are required above the transition midpoint of the DT test. The DT test shelf energy value has been demonstrated to provide direct correlation to K_{Ic} values for the low shelf condition (2). This condition is of particular importance for the case of high strength metals, including steels, titanium, and aluminum alloys.

REFERENCES

1. Pellini, W.S., Goode, R.J., Puzak, P.P., Lange, E.A., and Huber, R.W., "Review of Concepts and Status of Procedures for Fracture-Safe Design of Complex Welded Structures Involving Metals of Low to Ultra-High Strength Levels," NRL Report 6300, June 1965

2. Pellini, W.S., "Advances in Fracture Toughness Characterization Procedures and in Quantitative Interpretations to Fracture-Safe Design for Structural Steels," NRL Report 6713, Apr 3, 1968; Welding Res. Council Bull. 130 (1968)

3. Pellini, W.S., and Puzak, P.P., "Fracture Analysis Diagram Procedures for the Fracture-Safe Engineering Design of Steel Structures," NRL Report 5920, Mar. 15, 1963; Welding Res. Council Bull. 88 (1963)

4. Loss, F.J., and Pellini, W.S., "Dynamic Tear Test Definition of the Temperature Transition from Linear Elastic to Gross Strain Fracture Conditions," NRL Report 6787, Nov. 29, 1968; ASME Winter Annual Meeting, Dec 1-5, 1968, Paper 68-WA/ER-1

5. Pellini, W.S., and Puzak, P.P., "Practical Considerations in Applying Laboratory Fracture Test Criteria to the Fracture-Safe Design of Pressure Vessels," NRL Report 6030, Nov. 6, 1963

6. "HSST Program - Semi-Annual Progress Report for Period Ending February 29, 1968," ORNL-4315, Oak Ridge National Laboratory, Oct 1968

7. Wessel, E.T., "Linear Elastic Fracture Mechanics for Welded Steel Pressure Vessels: Material Property Considerations," Symposium on Fracture Toughness Concepts for Weldable Structural Steels, Culcheth, England, Apr 29-30, 1969

8. Loss, F.J., and Krafft, J.M., unpublished NRL data

9. Shoemaker, A.K., and Rolfe, S.T., "The Static and Dynamic Low-Temperature Crack-Toughness Performance of Seven Structural Steels," Eng. Fracture Mech., pending publication

10. Pellini, W.S., and Loss, F.J., "Integration of Metallurgical and Fracture Mechanics Concepts of Transition Temperature Factors Relating to Fracture-Safe Design for Structural Steels," NRL Report 6900, Feb. 17, 1969; Welding Res. Council Bull. 141 (1969)

11. Irwin, G.R., Krafft, J.M., Paris, P.C., and Wells, A.A., "Basic Aspects of Crack Growth and Fracture," NRL Report 6598, Nov. 1967; Whitman, G.D., Robinson, G.C., Jr., and Savolainen, A.W., editors, "Technology of Steel Pressure Vessels for Water-Cooled Nuclear Reactors," ORNL-NSIC-21, Oak Ridge National Laboratory, Dec. 1967

12. Smith, F.W., Emery, A.F., and Kobayashi, A.S., "Stress Intensity Factors for Semi-circular Cracks," J. Appl. Mech., Trans. ASME Ser. E, 34:953 (1967)

13. Puzak, P.P., and Babecki, A.J., "Normalization Procedures for the NRL Drop Weight Test," Welding J. Res. Suppl., May 1959

Security Classification

DOCUMENT CONTROL DATA - R & D

Security classification of title, body of abstract and indexing annotation must be entered when the overall report is classified)

1. ORIGINATING ACTIVITY (Corporate author) Naval Research Laboratory Washington, D.C., 20390	2a. REPORT SECURITY CLASSIFICATION UNCLASSIFIED 2b. GROUP

3. REPORT TITLE

COUPLING OF FRACTURE MECHANICS AND TRANSITION TEMPERATURE APPROACHES TO FRACTURE-SAFE DESIGN

4. DESCRIPTIVE NOTES (Type of report and inclusive dates)

Interim report; work is continuing.

5. AUTHOR(S) (First name, middle initial, last name)

F.J. Loss and W.S. Pellini

6. REPORT DATE April 14, 1969	7a. TOTAL NO. OF PAGES 32	7b. NO. OF REFS 13
8a. CONTRACT OR GRANT NO. NRL Problems M01-25-M01-14 b. PROJECT NO. RR 007-01-46-5409 c. AEC-83Y-80507V d. RR 007-01-46-5432	9a. ORIGINATOR'S REPORT NUMBER(S) NRL Report 6913 9b. OTHER REPORT NO(S) (Any other numbers that may be assigned this report)	

10. DISTRIBUTION STATEMENT

This document has been approved for public release and sale; its distribution is unlimited

11. SUPPLEMENTARY NOTES Also sponsored by the U.S. Atomic Energy Commission	12. SPONSORING MILITARY ACTIVITY Department of the Navy (Office of Naval Research), Washington, D.C., 20360; Atomic Energy Commission, Washington, D.C.20526

13. ABSTRACT

The effect of mechanical constraint on the transition temperature features for steels of thick section is examined in the framework of linear elastic fracture mechanics K_{Ic} and K_{Id} tests and the Dynamic Tear (DT) test. It is demonstrated that steels of fracture toughness and yield strength levels representative of the A533-B type continue to exhibit a transition to high fracture toughness in thick sections. The distinguishing feature of thick sections is a size effect involving a shift of the transition temperature midpoint on the order of 60°F. The DT test defines a limiting transition temperature region, which can be divided into three parts: a low temperature regime in which plane strain fracture mechanics is applicable, a higher temperature regime which is beyond the limits of fracture mechanics definition and is relatable to crack arrest conditions of the FTE type, and a final regime involving large plastic deformation in association with the fracture. The relatively narrow temperature span of the plane strain regime above the NDT temperature indicates practical difficulties in the direct application of fracture mechanics tests due to requirements for K_{Ic} and K_{Id} test specimens of large dimensions. A practical solution to the use of fracture mechanics principles may be obtained by considering the temperature-dependence aspects of the K_{Ic} and K_{Id} parameters. In general, the applicability of this approach is limited to temperatures below the FTE. If structural operation cannot be confined to temperatures above FTE, the Fracture Analysis Diagram (FAD) procedure, which is now extended to thick sections, is recommended as the best available engineering approach. The Drop Weight-NDT and FAD procedures are analyzed in terms of fracture mechanics aspects.

DD FORM 1 NOV 65 1473 (PAGE 1)

S/N 0101-807-6801

Security Classification

Security Classification

14 KEY WORDS	LINK A ROLE	LINK A WT	LINK B ROLE	LINK B WT	LINK C ROLE	LINK C WT
Engineering fracture mechanics						
Fracture toughness tests						
Fracture mechanics tests						
Fracture-safe design						
Structural steels						
Engineering fracture tests						
Thick section steels						
Design applications of fracture tests						
Interpretations of fracture mechanics theory to engineering design						
Steels for reactor technology						
Transition temperature for steels						
Micromechanics of cleavage fracture						

DD FORM 1 NOV 65 1473 (BACK)
(PAGE 2)

Security Classification